J. Chem. Thermodynamics 62 (2013) 130–141

Contents lists available at SciVerse ScienceDirect

J. Chem. Thermodynamics

journal homepage: www.elsevier.com/locate/jct

Density, refraction index and vapor–liquid equilibria of N-methyl-2-hydroxyethylammonium butyrate plus (methyl acetate or ethyl acetate or propyl acetate) at several temperatures

V.H. Alvarez [a], S. Mattedi [b], M. Aznar [c,*]

[a] Department of Agricultural, Food and Nutritional Science, University of Alberta, Edmonton, AB, Canada T6G 2P5
[b] Chemical Engineering Department, Polytechnic School, Federal University of Bahia (UFBA), 40210-630 Salvador-BA, Brazil
[c] School of Chemical Engineering, State University of Campinas (UNICAMP), P.O. Box 6066, 13083-970 Campinas-SP, Brazil

ARTICLE INFO

Article history:
Received 31 August 2012
Received in revised form 20 February 2013
Accepted 25 February 2013
Available online 4 March 2013

Keywords:
Ionic liquid
Binary mixtures
Density
Refraction index
Vapor–liquid equilibrium
COSMO-SAC

ABSTRACT

This paper reports the densities, refraction indices, and vapor liquid equilibria for binary systems ester + N-methyl-2-hydroxyethylammonium butyrate (m-2-HEAB): methyl acetate (1) + m-2-HEAB (2), ethyl acetate (1) + m-2-HEAB and propyl acetate (1) + m-2-HEAB (2). The excess molar volumes, deviations in the refraction index, apparent molar volumes, and thermal expansion coefficients for the binary systems were fitted to polynomial equations. The Peng–Robinson equation of state, coupled with the Wong–Sandler mixing rule, is used to describe the experimental data. Since the predictive activity coefficient model COSMO-SAC is used in the Wong–Sandler mixing rule, the resulting thermodynamic model is a completely predictive one. The prediction results for the density and for the vapor–liquid equilibria have a deviation lower than 1.0% and 1.1%, respectively.

1. Introduction

Actually, organic esters are important intermediates in chemical and pharmaceutical industries, and they are mostly produced by acid-catalyzed esterification reactions [1]. Various mineral acids have been used as catalysts for esterification, but they are extremely corrosive and need to be neutralized at the end of the reaction. Many acid-catalyzed organic reactions based on ionic liquids have been reported, among which esterifications are a hot topic [2]. Furthermore, at the end of the reaction, a direct liquid–liquid separation or distillation of the esters compounds from the reaction mixture appears very attractive in the case of derivatives that are volatile enough. Besides, the ionic liquid could be recycled after separation and purification stages.

By the accepted definition, room-temperature ionic liquids are salts that are liquids below 373 K, which are considered as potential substitutes to many traditional organic solvents in reaction and separation processes [3,4]. In spite of their importance and interest, accurate values for many of the fundamental physical–chemical properties of these compounds are either scarce or absent. In order to design any process involving ionic liquids in industrial scale, it is necessary to know several physical properties, including density and vapor–liquid equilibria in mixtures including ionic liquids. Since it is impossible to measure all the possible combinations of systems, it is necessary to make measurements on selective systems to provide results that can be used to develop correlations and predictive methods.

Most of the studies concerning ionic liquids have been based on the imidazolium cation and, to a lesser extent, on the alkyl pyridiniums and trialkylamines [5]. On the other hand, protic ionic liquids (PILs) have received limited attention from the academia, despite that the first PIL synthesized was the ethanolammonium nitrate, reported by Gabriel and Weiner in 1882 [6]. These PILs are produced by a stoichiometric acid–base Brønsted reaction and their main difference, compared to aprotic ionic liquids (AILs), is the presence of at least one proton, which is/are able to promote extensive hydrogen bonding [7]. Recently, some work has been reported on the synthesis, physicochemical and structural characterization of PILs. Bicak [8] synthesized the 2-hydroxyethylammonium formate (2-HEAF), an ionic liquid formed by the neutralization of monoethanolamine with formic acid. Greaves *et al.* [9] proposed different PILs from primary amines and organic and inorganic acids. Cota *et al.* [10], Kurnia *et al.* [11] and Alvarez *et al.* [12] synthesized several of these ionic liquids by modifying the aliphatic chain of the organic acid and/or using secondary and tertiary hydroxyamines. There were also studies that use PILs in catalytic reactions and on the interaction with hydroxilic

* Corresponding author. Tel.: +55 19 35213962; fax: +55 19 35213965.
E-mail address: maznar@feq.unicamp.br (M. Aznar).

0021-9614/$ - see front matter © 2013 Elsevier Ltd. All rights reserved.
http://dx.doi.org/10.1016/j.jct.2013.02.022

TABLE 1
Purity, water content by mass, w_{H2O}, and density, ρ, of pure components at $T = 298.15$ K and $p = 101.3$ kPa.

Compound	Source	Purification method	Mass fraction purity	Mass fraction w_{H2O} ($\times 10^2$)[a]	ρ (g · cm^{-3})	
					Exp	Lit
Methyl acetate	S-A[c]	None	>0.998[c]	<0.05	0.92682	0.9282[e]
Ethyl acetate	S-A[c]	None	>0.999[c]	<0.03	0.89490	0.8928[e]
Propyl acetate	S-A[c]	None	>0.995[c]	<0.5	0.88261	0.8823[e]
m-2-HEAB[b]	Synthesized	Vacuum heating	>0.980[d]	<0.1	1.03394	1.0392[f]

Standard uncertainties u are $u(\rho) = 0.00005$ g · cm^{-3} and $u(T) = 0.01$ K.
[a] Measured by Karl Fisher titration.
[b] m-2-HEAB = N-methyl-2-hydroxyethylammonium butyrate.
[c] Sigma–Aldrich.
[d] Measured by NMR method.
[e] Reference [16].
[f] Reference [12].

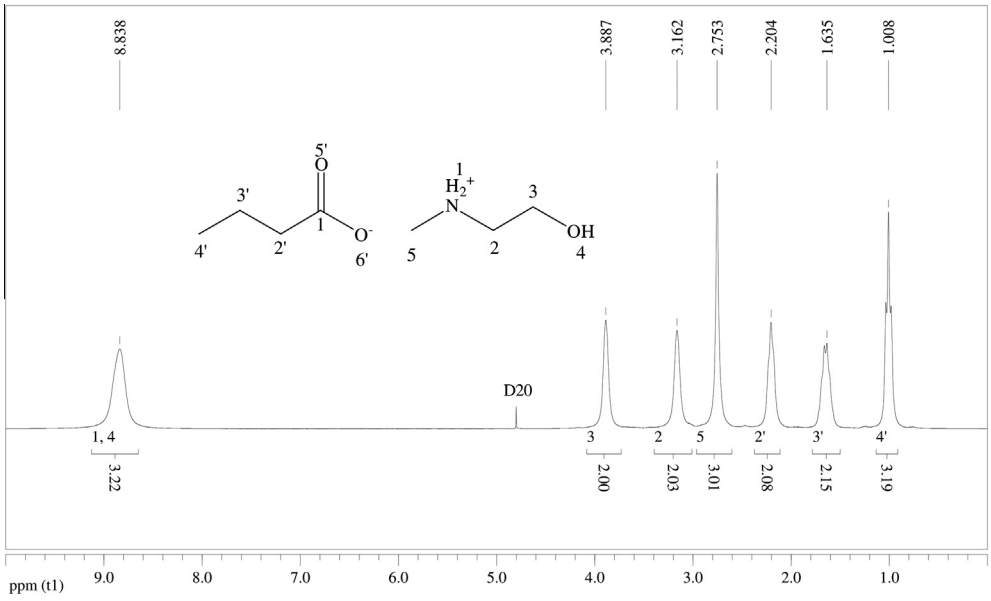

FIGURE 1. 1D hydrogen spectrum for m-2-HEAB.

solvents, showing that 2-HEAF is soluble in water, ethanol and methanol in all the concentration range [13]. Moreover, a relevant aspect, few times considered in the application of ionic liquids and the environment, is their potential toxicity. This issue has not been sufficiently studied, especially taking into account the need of this information to fulfill the REACH (Registration, Evaluation, Authorization and Restriction of Chemical Substances) requirements (UE) and so, allowing the assessment of hygiene and safety issues derived from their manufacture, use, and transport. Specifically about PILs from hydroxyamines and organic acids, the first results highlight that total biodegradation and low toxicity are intrinsic characteristics of this family of ionic liquids [14,15].

In this work, experimental density and refraction index data of pure protic ionic liquid N-methyl-2-hydroxyethylammonium butyrate (m-2-HEAB) have been measured at several temperatures. Also, experimental density, refraction index and vapor–liquid equilibrium (VLE) data over the whole composition range for binary mixtures methyl acetate (1) + m-2-HEAB (2), ethyl acetate (1) + m-2-HEAB (2) and propyl acetate (1) + m-2-HEAB (2) have been determined at 101.3 kPa. Thermal expansion coefficients, excess molar volumes, and deviations in the refraction index were calculated from experimental data. The Peng–Robinson equation of state, coupled with the Wong–Sandler mixing rule, was used to describe the experimental data. Since the predictive activity coefficient model COSMO-SAC was used in the Wong–Sandler mixing rule, the resulting thermodynamic model was a completely predictive one. The prediction results for the density and for the vapor–liquid equilibria had a deviation lower than 1.0% and 1.1%, respectively.

2. Experimental

2.1. Chemicals

The esters were supplied by Sigma–Aldrich, with purity higher than 99.0%, and were degassed ultrasonically.

2.2. Synthesis

N-methyl-2-hydroxyethylammonium butyrate was prepared according to the procedure by Alvarez *et al.* [12], slightly modified. Butanoic acid was added dropwise to a known amount of 2-(methylamino)ethanol and cooled in an ice bath under nitrogen in order to maintain the reaction temperature below 283.15 K, since the reaction is exothermic. The reaction mixture was stirred at room temperature for 5 h and the progress of the reaction was monitored by refraction index measurements. The ionic liquid N-methyl-2-hydroxyethylammonium butyrate obtained was dried

TABLE 2
Density and excess volume for the binary mixtures esters (1) + m-2-HEAB (2) at p = 101.3 kPa.

Methyl acetate + m-2-HEAB (288.15 K)			Ethyl acetate + m-2-HEAB (303.15 K)			Propyl acetate + m-2-HEAB (313.15 K)		
x_1	ρ/g · cm^{-3}	V^E/cm^3 · mol^{-1}	x_1	ρ/g · cm^{-3}	V^E/cm^3 · mol^{-1}	x_1	ρ/g · cm^{-3}	V^E/cm^3 · mol^{-1}
0.0000	1.0392	0.0001	0.0000	1.03587	0.0000	0.0000	1.02914	0.0000
0.0454	1.0298	0.7922	0.0454	1.02624	0.8080	0.0785	1.01332	0.9322
0.0956	1.0259	0.6434	0.0956	1.02232	0.6510	0.1247	1.00937	0.6252
0.1990	1.0173	0.3637	0.1990	1.01358	0.3460	0.2070	0.99976	0.4202
0.2901	1.0086	0.1619	0.2901	1.00461	0.1635	0.3035	0.98989	−0.1133
0.4120	0.9970	−0.2466	0.4120	0.99258	−0.2320	0.4177	0.97759	−0.7700
0.5070	0.9859	−0.4147	0.5070	0.98119	−0.4054	0.5088	0.96473	−0.9609
0.6018	0.9718	−0.3436	0.6018	0.96706	−0.3654	0.6042	0.94838	−0.8692
0.7039	0.9554	−0.3068	0.7039	0.95035	−0.3235	0.6960	0.93130	−0.7187
0.8031	0.9369	−0.1714	0.8031	0.93153	−0.1807	0.7939	0.91241	−0.6133
0.8998	0.9174	−0.0782	0.8998	0.91157	−0.0795	0.8936	0.89100	−0.3774
0.9497	0.9066	−0.0517	0.9497	0.90062	−0.0494	0.9454	0.87887	−0.1920
1.0000	0.8949	0.0000	1.0000	0.88876	0.0000	1.0000	0.86570	0.0000

Standard uncertainties u are $u(x) = 0.0007$, $u(\rho) = 0.00005$ and $u(T) = 0.01$ K.

by heating to (343.15 to 353.15) K and stirring under high vacuum (0.2 kPa) for 48 h. Its purity was ascertained as 98% mass fraction by NMR analysis.

The ionic liquid was kept in bottles with nitrogen gas. In order to reduce the water content (lower than 0.1% mass fraction, determined using a Mettler Toledo 756 Karl Fisher titrator), vacuum (0.2 Pa) and moderate temperature (343.15 K) were applied for several days, always immediately prior to their use.

Table 1 shows a comparison between experimental and literature data of the pure components at 298.15 K. The differences between experimental and literature data for pure m-2-HEAB can be due the water content, since the physical properties are strongly dependent of this.

2.3. Apparatus and procedure

Samples were prepared by introducing with a syringe known masses of the pure liquids into stoppered bottles, in an inert-atmosphere glove box, using a Mettler AX-205 Delta Range analytical balance, with a precision of $\pm 10^{-4}$ g. A glove box was used in order to prevent the water absorption by the ionic liquid. Densities were measured using an Anton Paar DMA 4000 digital vibrating-tube densimeter. The repeatability and the uncertainty in experimental measurement have been found to be lower than $\pm 5 \cdot 10^{-5}$ g · cm^{-3} for the density. The DMA 4000 automatically corrects the influence of viscosity on the measured density.

Refraction indices were determined using an automatic Mettler Toledo D4 refractometer with a resolution of $\pm 10^{-4}$ and an uncertainty in the experimental measurements of $\pm 2 \cdot 10^{-4}$.

The VLE data were measured using a glass Fischer 602 D Labodest (vapor + liquid) equilibrium still. The temperature was measured by a Pt100 platinum sensor with an uncertainty of ±0.1 K. For the pressure measurement, a differential U-tube glycerol manometer was used, with an uncertainty of ±0.01 kPa. Nitrogen was injected into the still to maintain a constant pressure of 101.32 kPa, in agreement with the local atmospheric pressure. During the operation, a liquid binary mixture of ester + m-2-HEAB was placed inside the boiling chamber and heated. The (vapor + liquid) in the boiling chamber was carried upward to the equilibrium chamber, where the vapor and liquid phases were separated after flowing directly along the thermometer stem. The vapor was condensed in the condenser and went to the mixing chamber. The equilibrium was usually reached in about 30–60 min, as indicated by the constant boiling temperature. The system was maintained in equilibrium for about 30 min, and then samples of the vapor and liquid were taken out by syringes. The compositions of the vapor and liquid phases were determined by refractometric analysis. The refraction index of both phases was measured at 288.2 K and the results were compared with samples of known composition, through an inverse interpolation.

3. Modeling

3.1. Volumetric and optical properties

The density and refraction index for the mixtures were correlated by:

TABLE 3
Refraction index and deviations for the binary mixtures esters (1) + m-2-HEAB(2) at p = 101.3 kPa.

Methyl acetate + m-2-HEAB (288.15 K)			Ethyl acetate + m-2-HEAB (303.15 K)			Propyl acetate + m-2-HEAB (313.15 K)		
x_1	n_D	δn_D	x_1	n_D	δn_D	x_1	n_D	δn_D
1.0000	1.3650	0.0000	1.0000	1.3672	0.0000	1.0000	1.3741	0.0000
0.9483	1.3746	0.0048	0.9497	1.3746	0.0031	0.9454	1.3809	0.0027
0.8979	1.3833	0.0088	0.8998	1.3812	0.0054	0.8936	1.3870	0.0048
0.7912	1.3996	0.0152	0.8031	1.3949	0.0107	0.7939	1.3991	0.0093
0.6898	1.4130	0.0191	0.7039	1.4055	0.0128	0.6960	1.4068	0.0095
0.5928	1.4232	0.0203	0.6018	1.4161	0.0146	0.6042	1.4146	0.0103
0.4973	1.4327	0.0210	0.5070	1.4246	0.0149	0.5088	1.4222	0.0106
0.3983	1.4399	0.0190	0.4120	1.4324	0.0145	0.4177	1.4288	0.0103
0.3079	1.4449	0.0056	0.2901	1.4411	0.0127	0.3035	1.4365	0.0092
0.2074	1.4509	0.0123	0.1990	1.4472	0.0109	0.2070	1.4417	0.0071
0.1097	1.4556	0.0079	0.0956	1.4511	0.0059	0.1247	1.4457	0.0048
0.0646	1.4558	0.0039	0.0454	1.4533	0.0038	0.0785	1.4483	0.0039
0.0000	1.4579	0.0000	0.0000	1.4534	0.0000	0.0000	1.4504	0.0000

Standard uncertainties u are $u(x) = 0.0007$, $u(n_D) = 0.0002$ and $u(T) = 0.01$ K.

TABLE 4
Fitting parameters and root mean square deviations for density and refraction index of binary mixtures by equation (1).

	Methyl acetate + m-2-HEAB		Ethyl acetate + m-2-HEAB		Propyl acetate + m-2-HEAB	
	$\rho/(g \cdot cm^{-3})$	n_D	$\rho/(g \cdot cm^{-3})$	n_D	$\rho/(g \cdot cm^{-3})$	n_D
B_{00}	1.232E+00	−2.777E+04	1.199E+00	−3.073E+04	1.191E+00	−3.279E+04
B_{01}	−6.045E−04	−9.538E+01	−4.133E−04	−1.004E+02	−3.631E−04	−1.037E+02
B_{02}	−1.288E−07	6.655E−01	−4.314E−07	6.656E−01	−4.988E−07	6.656E−01
B_{10}	−4.042E−02	−2.777E+04	6.744E−01	−3.073E+04	1.153E−01	−3.279E+04
B_{11}	−3.270E−04	−9.538E+01	−5.009E−03	−1.004E+02	−1.418E−03	−1.037E+02
B_{12}	2.275E−09	6.655E−01	7.651E−06	6.656E−01	1.437E−06	6.656E−01
B_{20}	−4.289E−01	−2.777E+04	2.726E+00	−3.073E+04	−7.005E−01	−3.279E+04
B_{21}	5.014E−03	−9.538E+01	−1.493E−02	−1.004E+02	5.699E−03	−1.037E+02
B_{22}	−8.910E−06	6.655E−01	2.216E−05	6.656E−01	−7.503E−06	6.656E−01
B_{30}	1.038E+00	−2.777E+04	−1.029E+01	−3.073E+04	3.092E−01	−3.279E+04
B_{31}	−9.772E−03	−9.539E+01	6.185E−02	−1.004E+02	−3.651E−03	−1.037E+02
B_{32}	1.697E−05	6.655E−01	−9.657E−05	6.656E−01	2.715E−06	6.656E−01
B_{40}	−5.938E−01		6.943E+00		2.368E−01	
B_{41}	5.138E−03		−4.266E−02		−9.480E−04	
B_{42}	−9.241E−06		6.703E−05		3.117E−06	
s	$8.9 \cdot 10^{-4}$	3.9	$9.2 \cdot 10^{-4}$	8.5	$1.0 \cdot 10^{-3}$	1.45

ρ: density.
n_D: refractive index.
B_{ij}: the fitting parameters of equation (1).
s: standard deviation between experimental and calculated values.

$$Z = \sum_{i=0}^{p}\left(\left(\sum_{j=0}^{q} B_{ij}T^j\right)x_1^i\right), \tag{1}$$

where Z is the density or refraction index of the mixture, x_1 is the mole fraction of the solvent, p and q are the polynomial degrees, B_{ij} are the fitting parameters, and T is the absolute temperature.

The excess molar volumes (V^E) and deviations in the refraction index (δn_D) were calculated from experimental values as follows:

$$V^E = \sum_{i=1}^{N} x_i M_i\left(\frac{1}{\rho} - \frac{1}{\rho_i}\right), \tag{2}$$

$$\delta n_D = n_D - \sum_{i=1}^{N} x_i n_{Di}, \tag{3}$$

where N is the number of compounds in the mixture; x_i is mole fraction; M_i denotes molar mass; ρ_i is the density of the pure compound i; ρ is the density of the mixture; n_D and n_{Di} are the refraction index of the mixture and the refraction index of the pure components, respectively. These derived properties were fitted to a Redlich–Kister-type equation:

$$Q_{12} = x_1x_2\sum_{i=0}^{p}\left(\left(\sum_{j=0}^{q} C_{ij}T^j\right)(x_1 - x_2)^i\right), \tag{4}$$

where Q_{12} is V^E or $\delta\kappa_S$ and the other variables are the same as above.

The apparent molar volume (ϕ_V) for the binary mixtures were calculated by:

$$\phi_V = 1000\left(\frac{\rho_1 - \rho}{m\rho_1\rho}\right) + \frac{M_2}{\rho_1}, \tag{5}$$

where ρ is the density of the mixture; ρ_1 is the density of the solvent; M_2 is the molar mass of ionic liquid; m is the molality of the solution. These derived values were correlated as a function of temperature and mole fraction by equation (1).

The thermal expansion coefficient (α_P) shows the temperature dependence of volume, and it is defined as:

$$\alpha_P = \frac{1}{V}\left(\frac{\partial V}{\partial T}\right)_P = -\left(\frac{\partial \ln\rho}{\partial T}\right)_P. \tag{6}$$

3.2. Vapor–liquid equilibria

The most common method used for the correlation of phase equilibria in mixtures at high and low pressure is the use of equations of state (EoS). The most common and industrially important EoS are the cubic equations derived from van der Waals EoS; among these, the Peng–Robinson EoS [17] has proven to combine the simplicity and accuracy required for the prediction and correlation of volumetric and thermodynamic properties of fluids, although there can be problems when applying the PR EoS to systems near the critical point.

Recently, Alvarez and Aznar [18] applied an extension of this approach to several supercritical fluid + ionic liquid systems, using the Peng–Robinson equation of state coupled with the Wong–Sandler mixing rule [19] using the UNIQUAC model [20] for G^E. This model used three adjustable parameters.

By using the Wong–Sandler mixing rule, any cubic EoS can be made predictive for mixtures, *i.e.*, without the need of any adjustable binary interaction parameter, when a predictive model for G^E is used. For example, G^E can be determined from the COSMO-SAC model [21], in which the activity coefficient γ_i of species i is calculated from the sum of the residual and combinatorial contributions:

$$\ln\gamma_i = \ln\gamma_i^{res} + \ln\gamma_i^{com}. \tag{7}$$

The residual part is calculated from a consideration of molecular solvation in a perfect conductor. The distribution of screening charges on the molecular surface, called the sigma profile, $p(\sigma)$, is first determined from quantum mechanical calculations. The molecular interactions in the liquid phase are assumed to be the sum of contributions of surface segment interactions through the screening charges. With these assumptions, the residual term takes the following form:

$$\ln\gamma_i^{res} = n_i\sum_{\sigma_m} p_i(\sigma_m)\ln[\Gamma_S(\sigma_m) - \Gamma_i(\sigma_m)], \tag{8}$$

where n_i is the number of surface segments contained in species i, $\Gamma_S(\sigma)$ is the activity coefficient of segment i (whose screening charge density is σ) in solution S (for which the probability of finding a segment of charge density σ be denoted $p_S(\sigma)$:

$$\ln \Gamma_S(\sigma_m) = -\ln\left\{\sum_{\sigma_n} p_S(\sigma_n)\Gamma_S(\sigma_n)\exp\left[\frac{-\Delta W(\sigma_m,\sigma_n)}{RT}\right]\right\}, \quad (9)$$

where $W(\sigma_m, \sigma_n)$ is the electrostatic interaction between two segments of charge density σ_m and σ_n. The Staverman–Guggenheim model is used for the combinatorial term:

$$\ln \gamma_i^{com} = \ln\frac{\Phi_i}{x_i} + \frac{z}{2} q_i \ln\frac{\theta_i}{\Phi_i} + l_i - \frac{\Phi_i}{x_i}\sum_j x_j l_j, \quad (10)$$

$$\Phi_i = \frac{r_i x_i}{\sum_j r_j x_j}, \qquad \theta_i = \frac{q_i x_i}{\sum_j q_j x_j}, \quad (11)$$

$$l_i = (z/2)(r_i - q_i) - (r_i - 1), \quad (12)$$

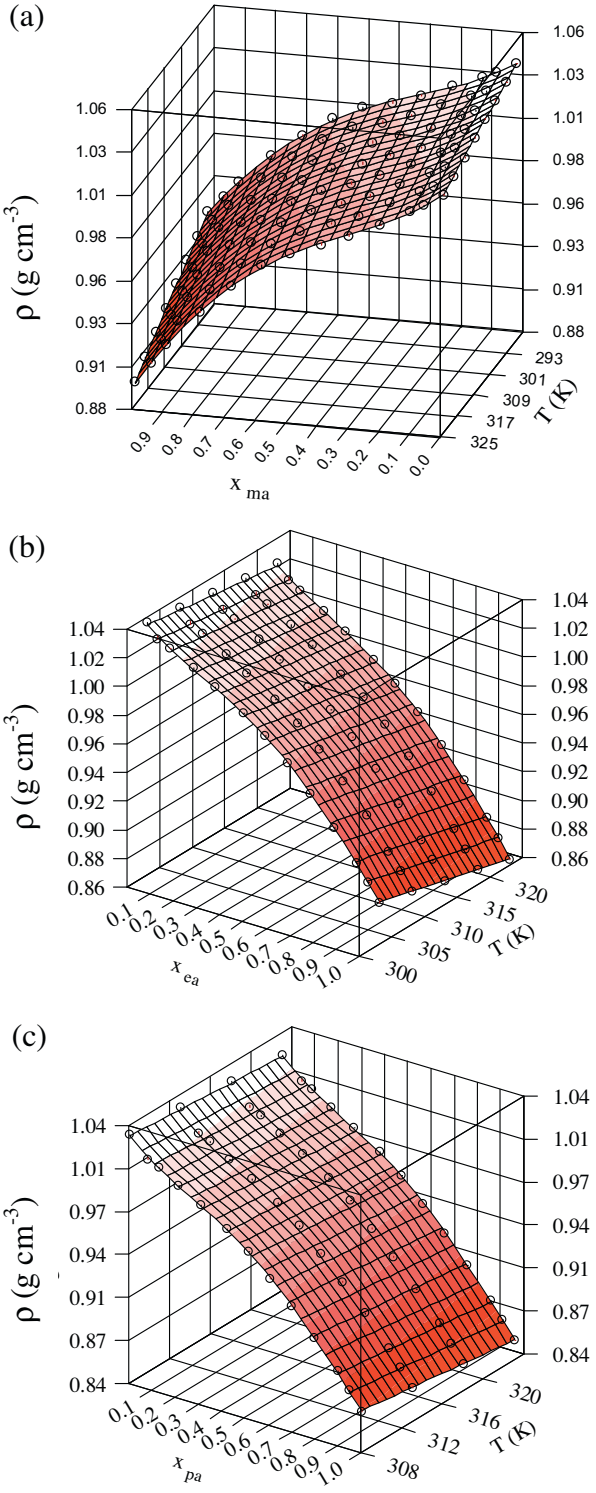

FIGURE 2. Density versus ester mole fraction and temperature: (a) methyl acetate + m-2-HEAB, (b) ethyl acetate + m-2-HEAB, (c) propyl acetate + m-2-HEAB.

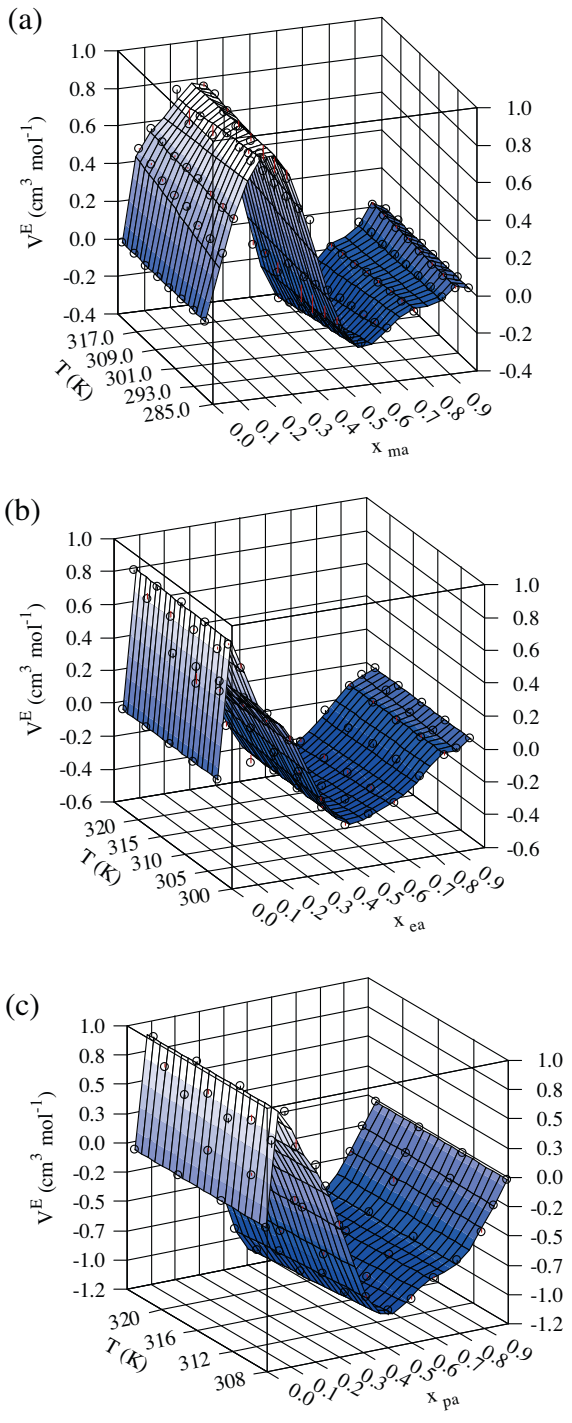

FIGURE 3. Excess molar volume versus ester mole fraction and temperature: (a) methyl acetate + m-2-HEAB, (b) ethyl acetate + m-2-HEAB, (c) propyl acetate + m-2-HEAB.

where θ_i is the surface area fraction, Φ_i is the volume fraction, z is the coordination number ($z = 10$), and r_i and q_i are the normalized volume and surface area parameters for species i.

3.3. Density predictions

The calculation of the molar volume of the mixture at a specific temperature and pressure can be predicted by an equation of state. The Peng–Robinson equation of state, coupled with the Wong–Sandler mixing rule using the predictive liquid activity coefficient model COSMO-SAC was used as thermodynamic model to predict the density. In the COSMO model, for each compound, the equilibrium molecular geometry is first determined by minimization of the molecular energy at 0 K. The next step for COSMO-SAC calculation is to estimate the volume of cavity (V_{COSMO}), the total number of segments (COSMO segments), and the sigma profile of each compound. The calculations were done using the quantum chemistry package DMol3 built in Accelrys Materials Studio v4.3 [22]. The sigma profile, $p(\sigma)$, is a file containing the probability of finding a surface segment with screening charge density, σ. The detailed settings for DMol3 can be found elsewhere [23] and, for the molecular description of the ionic liquid, the ion-pair approach [24] is used. The sigma profile of ionic liquids has been obtained for the molecule as a whole. The activity coefficient is then calculated [23]. The Peng–Robinson equation can be written in terms of the compressibility factor (Z) by:

$$Z^3 - (1 - B)Z^2 + (A - 3B^2 - 2B)Z - (AB - B^2 - B^3) = 0, \tag{13}$$

where A and B are given by:

$$A = \frac{a_m P}{(RT)^2}, \tag{14}$$

$$B = \frac{b_m P}{RT}, \tag{15}$$

where the constants a_m and b_m are expressed by mixing rules as functions of the concentration of the different components in the mixture. In this work, the Wong–Sandler mixing rules are used:

$$b_m = \frac{\sum_i \sum_j x_i x_j \left(b - \frac{a}{RT}\right)_{ij}}{1 - \sum_i \frac{x_i a_{ii}}{b_{ii} RT} - \frac{A^E_\infty}{\Omega RT}}, \tag{16}$$

$$a_m = b_m \left[\sum_i \frac{x_i a_{ii}}{b_{ii}} + \frac{A^E_\infty}{\Omega}\right], \tag{17}$$

$$\left(b - \frac{a}{RT}\right)_{ij} = \frac{(b_{ii} + b_{jj})}{2} - \frac{(1 - k_{ij})\sqrt{a_{ii} a_{jj}}}{RT}. \tag{18}$$

In these equations, k_{ij} is the adjustable interaction parameter, $\Omega = \ln(2^{1/2}-1)/2^{1/2}$ for the PR EoS, and A^E_∞, the excess Helmholtz energy at the limit of infinite pressure, is calculated using the COSMO-SAC activity coefficient model, while a_{ii} and b_{ii} are the EoS constants, defined as

$$a_{ii} = 0.457235 (RT_c/P_c)^2 [1 + F(1 - T_r^{0.5})],$$
$$F = 0.37464 + 1.54226\omega - 0.26992\omega^2, \tag{19}$$

$$b_{ii} = 0.077796 (RT_c/P_c), \tag{20}$$

where T_r is the reduced temperature, T_c is the critical temperature, P_c is the critical pressure, and ω is the Pitzer acentric factor.

Equation (13) yields one or three real roots, depending on the number of phases in the system. It was shown that this model provides an excellent representation of the vapor–liquid experimental data [18]. For the prediction of the liquid density, the root of interest is the smallest positive one. An equation of state does not necessarily yield the accurate volumetric behavior of fluids and their mixtures. Therefore, a correction of the volume translation can be adopted in the equation of state, to improve the volumetric behavior [25,26]. This correction is calculated as an ideal solution and assumed to be a good approximation for real solutions. This property may be exploited to improve the volume estimations made by the Peng–Robinson equation of state. Then, the correction value for each pure component (Δv_i) is given by the difference between the volume calculated by the thermodynamic model and the experimental volume:

$$\Delta v_i = V_{i,\mathrm{exp}} - V_{i,\mathrm{cal}}, \tag{21}$$

where $V_{i,cal}$ is the molar volume of the compound i calculated by the thermodynamic model, and $V_{i,exp}$ is the experimental molar volume of the compound i. Then, the volume of the mixture is obtained using the correction of the volume applied by

$$V = V_{\mathrm{cal}} + \sum_i \Delta v_i x_i, \tag{22}$$

where x_i is the liquid molar fraction of the pure compound i, V_{cal} is the liquid molar volume of the mixture calculated with the thermodynamic model, and V is the predicted corrected molar volume of the mixture.

3.4. Computation details

The vapor–liquid equilibrium (VLE) phase diagrams of three binary mixtures covering a wide range of temperature (313.15–403.15) K at 101 kPa are examined. The chosen systems have strong interactions between the species (esters and ionic liquid).

For each system, the VLE phase diagram is predicted by using the Peng–Robinson EoS with the Wong–Sandler/COSMO-SAC mixing rule. For a given liquid phase composition, the bubble point pressure calculation, as detailed by Michelsen and Mollerup [27], is performed to obtain the system pressure and the vapor phase compositions. In order to make the models predictive, the binary interaction parameters k_{ij} in the combining rules are set to zero.

For each compound, the equilibrium molecular geometry is first determined by minimization of the molecular energy at 0 K using the quantum chemistry package DMol3 implemented in Accelrys Materials Studio v4.3 [22]. A solvation calculation in a perfect conductor is then performed using the equilibrium geometry to obtain the surface screening charges on the compound. The detailed settings for DMol3 can be found elsewhere [21]. The activity coefficient is then calculated from the procedure above using an in-house program. Note that, for each species, the quantum mechanical part of this calculation, which may be time consuming, only has to be done once, regardless of the temperature and the composition of mixture needed. The absolute average error in pressure and vapor phase composition from the calculation is determined as:

$$|\Delta P|\% = \frac{100}{N} \sum_{i=1}^{N} \frac{|P_i^{\mathrm{cal}} - P_i^{\mathrm{exp}}|}{P_i^{\mathrm{exp}}}, \tag{23}$$

where N is the number of data point, superscripts *exp* and *cal* denote the values from experiment and our calculation, respectively.

4. Parameter estimation

In this work, the first approximation parameter estimation was performed using a genetic algorithm code, mMyGA [28] using a whole interval search. After that, the fitting parameters were best tuned using a non-linear optimization algorithm based on the Marquardt algorithm. The optimization used the minimization of

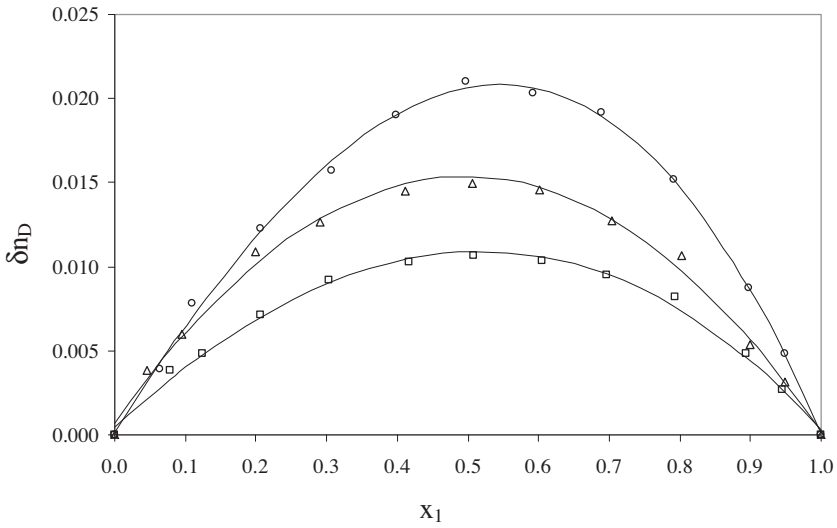

FIGURE 4. Deviations in the refraction index: methyl acetate (○), ethyl acetate (Δ), propyl acetate (□), fitted values by the Redlich–Kister model (solid line).

TABLE 5
Fitting parameters and root mean square deviations for excess molar volume and deviations of refraction index of binary mixtures by equation (4).

	Methyl acetate + m-2-HEAB		Ethyl acetate + m-2-HEAB		Propyl aceate + m-2-HEAB	
	$V^E/(cm^3 \cdot mol^{-1})$	δn_D	$V^E/(cm^3 \cdot mol^{-1})$	δn_D	$V^E/(cm^3 \cdot mol^{-1})$	δn_D
C_{00}	3.522E−01	8.358E−02	−1.410E+00	5.932E−02	5.642E+00	4.207E−02
C_{01}	−2.220E−03		−4.827E−04		−3.047E−02	
C_{10}	2.263E+01	2.046E−02	1.990E+01	3.731E−04	8.886E+00	−2.466E−03
C_{11}	−1.023E−01		−7.116E−02		−3.082E−02	
C_{20}	1.655E+01	−3.952E−02	3.372E+01	2.424E−02	−2.587E+01	2.265E−02
C_{21}	−5.146E−03		−7.384E−02		1.431E−01	
C_{30}	−1.615E+02	−2.684E−02	−2.016E+02	5.451E−03	−1.027E+02	4.328E−02
C_{31}	5.991E−01		6.189E−01		2.362E−01	
C_{40}	4.460E+01	1.754E−01	−4.874E+01	−2.229E−02	5.698E+01	−5.188E−02
C_{41}	−2.512E−01		6.217E−02		−3.290E−01	
C_{50}	2.592E+02	2.583E−02	4.773E+02	−2.330E−02	2.363E+02	−5.718E−02
C_{51}	−9.653E−01		−1.406E+00		−5.372E−01	
C_{60}	−1.085E+02	−1.643E−01	1.173E+01	1.010E−02	−3.227E+01	5.576E−02
C_{61}	4.374E−01		8.512E−02		2.633E−01	
C_{70}	−9.517E+01		−3.437E+02		−1.879E+02	
C_{71}	3.788E−01		9.433E−01		3.963E−01	
s	$3.6 \cdot 10^{-2}$	$3.7 \cdot 10^{-4}$	$2.6 \cdot 10^{-2}$	$4.0 \cdot 10^{-4}$	$2.9 \cdot 10^{-2}$	$1.4 \cdot 10^{-4}$

V^E: excess molar volumes.
δn_D: changes of refractive index.
C_{ij}: the fitting parameters of equation (4).
s: standard deviation between experimental and calculated values.

TABLE 6
Fitting parameters and standard deviations for apparent molar volume of binary mixtures by equation (1).

	Methyl acetate + m−2-HEAB ϕ_V $(cm^3 \cdot mol^{-1})$	Ethyl acetate + m-2-HEAB ϕ_V $(cm^3 \cdot mol^{-1})$	Propyl acetate + m-2-HEAB ϕ_V $(cm^3 \cdot mol^{-1})$
B_{00}	9.8281E+01	1.0224E+02	1.0922E+02
B_{01}	2.6069E−01	2.6788E−01	2.5270E−01
B_{10}	1.3203E+01	2.0294E+01	2.2280E+01
B_{11}	−6.2383E−02	−1.0195E−01	−1.1837E−01
B_{20}	1.2451E+01	−2.4410E+00	−1.2352E+01
B_{21}	−8.4847E−02	−4.3543E−02	−1.9032E−02
s	0.1	0.1	0.2

ϕ_V: apparent molar volume.
B_{ij}: the fitting parameters of equation (1).
s: standard deviation between experimental and calculated values.

the standard deviation (s) between experimental and calculated values, defined as:

$$s = \left[\sum_{i=1}^{N} \frac{(F_{exp} - F_{cal})_i^2}{N - m}\right]^{1/2}, \quad (24)$$

where N is the number of experimental points, m is the number of parameters in the curve fit, and F_{cal} and F_{exp} are the values of the property calculated by the model and obtained experimentally, respectively.

5. Results and discussion

The m-2-HEAB was synthesized and the 1D hydrogen spectrum was similar to that presented by Alvarez *et al.* [12], as can be seen in figure 1. The m-2-HEAB shows complete solubility in water, methanol and ethanol, and it is not soluble in some alkanes such as n-octane and n-dodecane. The humidity of the ionic liquid was determined by using a Mettler Toledo DL31 Karl Fischer titrator and shows moisture less than 900 ± 50 ppm of H_2O.

The m-2-HEAB ionic liquid shows complete solubility in methyl acetate, in ethyl acetate, and in propyl acetate from 288.15, 303.15, and 308.15 K, respectively. These data established the lower temperature where the liquids were miscible and thus where the excess properties could be determined.

5.1. Volumetric and optical properties

Densities and excess molar volumes of the binary mixtures methyl acetate (1) + m-2-HEAB (2), ethyl acetate (1) + m-2-HEAB (2) and propyl acetate (1) + m-2-HEAB (2) at 298.15 K and refraction indices and deviations in the refraction indices at atmospheric pressure are listed in tables 2 and 3. The complete data are presented in the Supplementary data. Table 4 contains the fitting parameters for density and refraction index by equation (1). Figure 2 shows density as a function of composition and temperature. This figure shows a similar behavior for the three binary mixtures. The increase of density is obtained by a decrease of temperature and an increase of ionic liquid composition. In all figures, the open points are the experimental data and the lines are the results for the model fitting.

Figures 3 and 4 show the experimental excess molar volume and deviations in the refraction index, respectively, as well as the fitted curves for binary mixtures ester + m-2-HEAB. Table 5 contains the fitting parameters for these properties. In figure 3a we can observe that the excess molar volumes show a minimum at $x_1 = 0.6$ for the methyl acetate + m-2-HEAB system and $x_1 = 0.5$ for the other two systems; besides, the methyl acetate + m-2-HEAB system presents a maximum at $x_1 = 0.25$ and $x_1 = 0.1$ for the other

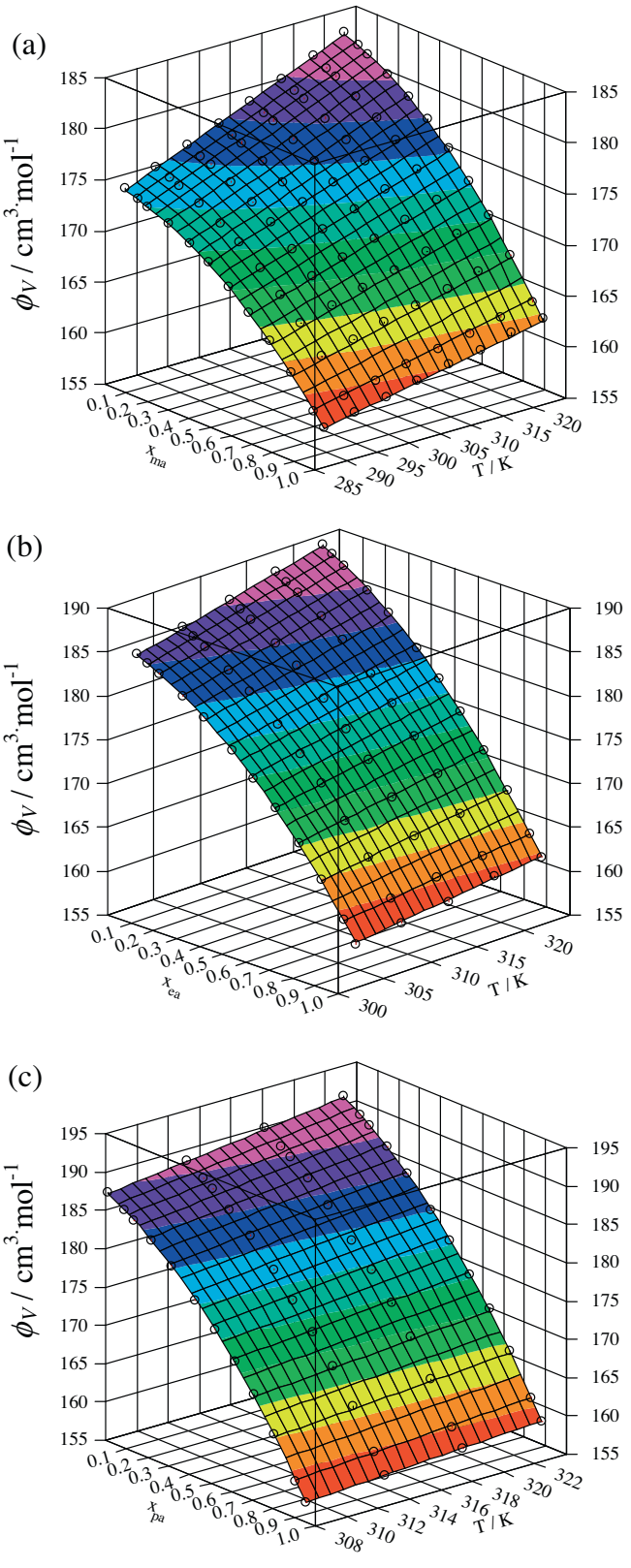

FIGURE 5. Apparent molar volume versus ester mole fraction and temperature: (a) methyl acetate + m-2-HEAB, (b) ethyl acetate + m-2-HEAB, (c) propyl acetate + m-2-HEAB.

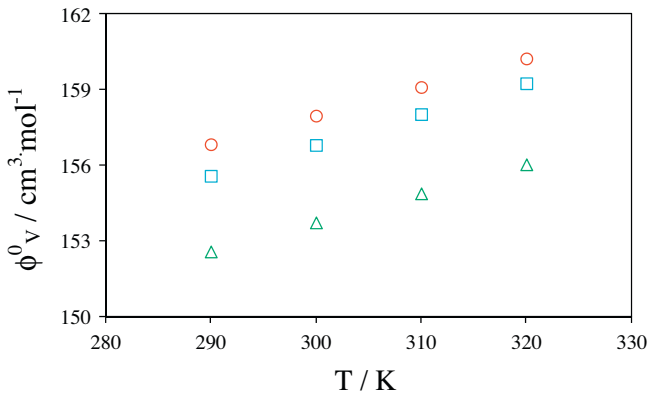

FIGURE 6. Apparent molar volume at ionic liquid infinite dilution versus temperature: methyl acetate (○), ethyl acetate (□) and propyl acetate (Δ).

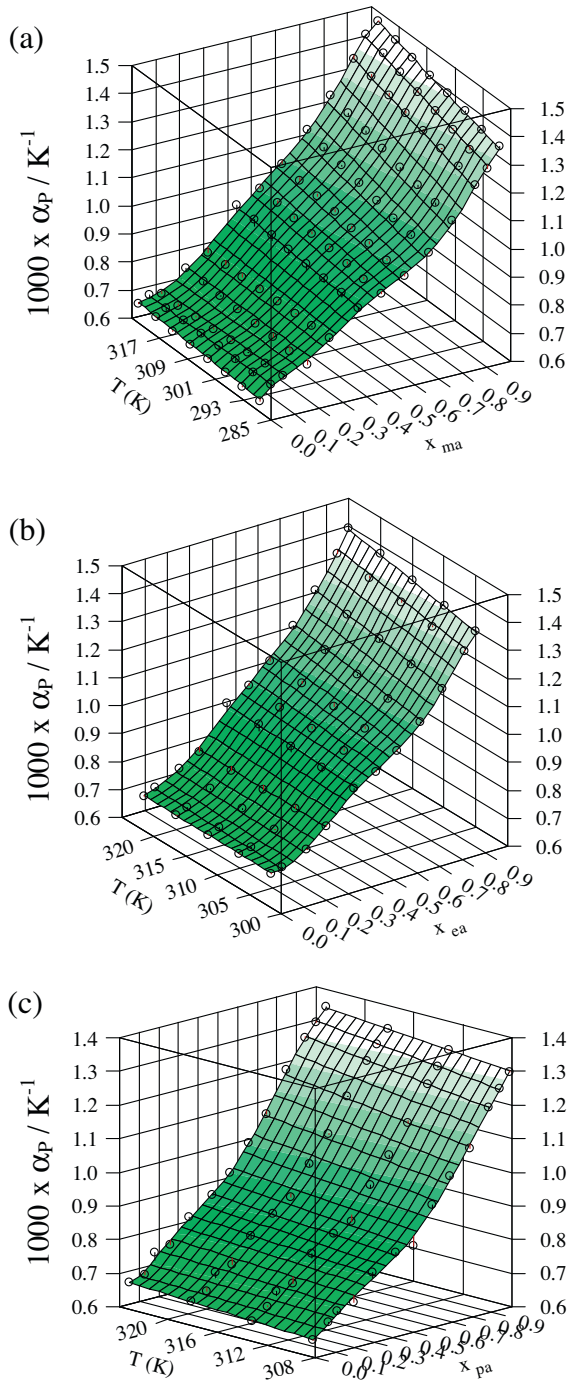

FIGURE 7. Thermal expansion coefficient versus ester mole fraction and temperature: (a) methyl acetate + m-2-HEAB, (b) ethyl acetate + m-2-HEAB, (c) propyl acetate + m-2-HEAB.

two systems. The minimum V^E could be due to hydrogen bonds between ester and ionic liquid. At higher concentrations of ester, in the methyl acetate + m-2-HEAB system we can observe a maximum that can be due to the dissociation of the ions in the ionic liquid. In the same way, low concentration of the ester breaks the self-associate ionic liquid to build a positive V^E. Also, a continuous addition of ester in the ionic liquid structure results in considerable decrease in the excess molar properties to more negative values to build association ionic liquid-ester, showing the polar effect of the molecules. In other cases, the increase of the alkyl chain in the ester results in an increase of the excess molar properties, showing the ability of the alkyl chain to fill the holes of the new structure ionic liquid-ester.

In figure 4, the refraction index deviations are positive values for the three systems, and the maximum lies at a mole fraction of approximately 0.6 for the methyl acetate + m-2-HEAB system and at 0.5 for the other two systems. According to Nakata and Sakurai [29], the sign of δn_D is opposite to that of V^E if the behavior of the refraction index is not too non-linear between n_{D1} and n_{D2}. In our mixtures this rule is truly fulfilled in all the cases.

The apparent molar volume data are given in the Supplementary data. Table 6 contains the fitting parameters for this property. Figure 5 shows that the apparent molar volume, ϕ_V, rises rapidly at low concentrations (below 30 mol · kg^{-1}), while at higher concentrations is almost constant (all three mixtures shown the same trend). Also, in the figures the properties increase with temperature at all concentrations.

The values for apparent molar volumes at infinite dilution ϕ_V^0 were obtained by extrapolation at ionic liquid infinite dilution ($x_1 \to 1$), based on Equation (1). The values of ϕ_V^0 for several temperatures are shown in figure 6. This figure shows that the apparent molar volume at infinite dilution for the methyl acetate mixture is greater than for the other mixtures and increases with the increasing of temperature.

The values for the thermal expansion coefficient are shown in the Supplementary data and the behavior is shown in figure 7. The value deduced for α_P is particularly sensitive to the type of mathematical function used to fit the density data. The fit can be done with a linear function; however, subtle effects stem from the non-linear behavior of most fluids, and therefore a piece of information may be lost. In these figures, the ionic liquid shows a stable value of thermal expansion coefficient with the increase of temperature, a different behavior for the binary mixtures and esters solvents. For the binary mixtures, the thermal expansion coefficient increases with the rise of the temperature and concentration of the ester. This behavior shows a very polar attraction among the high ordering molecules of the ionic liquid.

5.2. Density predictions

Figure 8 compares the σ-profile for m-2-HEAB, methyl acetate, ethyl acetate, and propyl acetate compounds. The σ-profile of these compounds can be qualitatively divided in three main regions, which are separated in figure 8 by two vertical lines located at the cutoff values for the hydrogen bond donor ($\sigma_{HB} < -0.0084$ e · Å^{-2}) and acceptor ($\sigma_{HB} > 0.0084$ e · Å^{-2}) group [21]. For m-2-HEAB, the σ-profile reveals to be broad such as the σ-profiles of the hydroxylic solvents. Also, the σ-profile of this ionic liquid is dominated by a huge peak of slightly negative screening charge density at $\sigma = -0.003$, which is due to polarization of –CH_2– groups by the ammonium-hydrogen, hydroxyl-hydrogen and oxygen atoms. The two peaks about 0.009 and 0.012 corresponds to the negatively charged –COO^- and lone pairs of the oxygen in the –OH groups, respectively. Considering the high-polarity region $\sigma_{HB} > 0.0084$ e · Å^{-2}, these groups can be considered as hydrogen-bond acceptor groups [21,24]. On the left hand side of the histogram, it can be observed two low peaks at values lower than the cutoff -0.0084 e · Å^{-2}, which are affected by the alkyl chain. These peaks are related to the ammonium-hydrogen and hydroxyl-hydrogen; they may contribute to hydrogen bonds as donors. Finally, the distribution of the charge densities around zero (-0.0084 e · Å$^{-2} < \sigma < 0.0084$ e · Å^{-2}) corresponds to the non-polar alkyl groups of the cation, being those for positive and negative signs assigned to carbon and hydrogen atoms, respectively. Figure 8 shows that the higher number of carbon atoms in alkyl chain implies the increasing of the area below each histogram of charge densities around the non-polar area (water < methanol < etha-

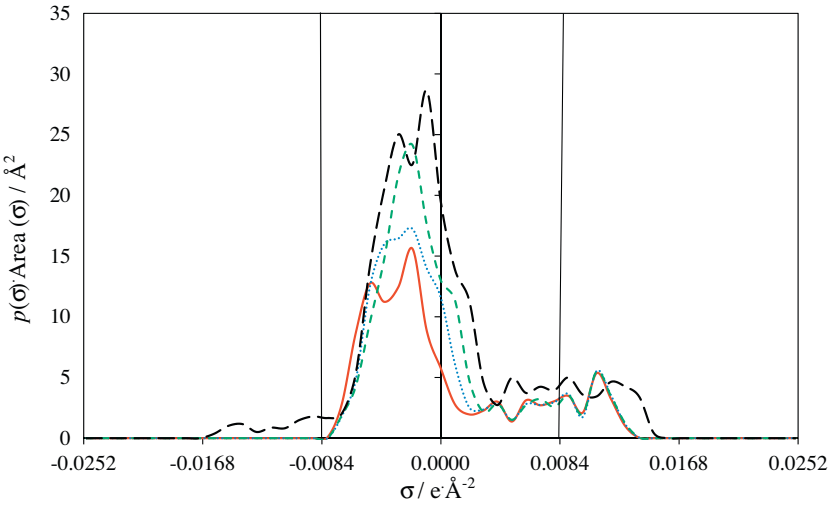

FIGURE 8. Sigma profiles employed for m-2-HEAB (— —), methyl acetate (—), ethyl acetate (···), and propyl acetate (--). Note that, due to the definition as conductor screening charges, electrostatically positive parts of the molecules have negative σ and vice versa.

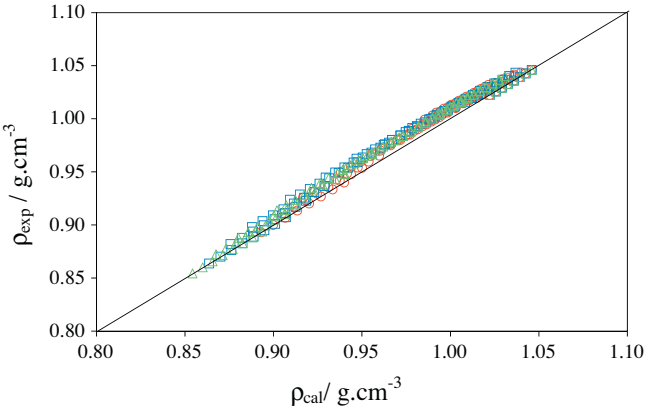

FIGURE 9. Comparison of experimental and PR-WS/COSMO-SAC model predicted values of density ($g \cdot cm^{-3}$) for binary mixtures: methyl acetate + m-2-HEAB (○), ethyl acetate + m-2-HEAB (□) and propyl acetate + m-2-HEAB (Δ) in the whole composition interval.

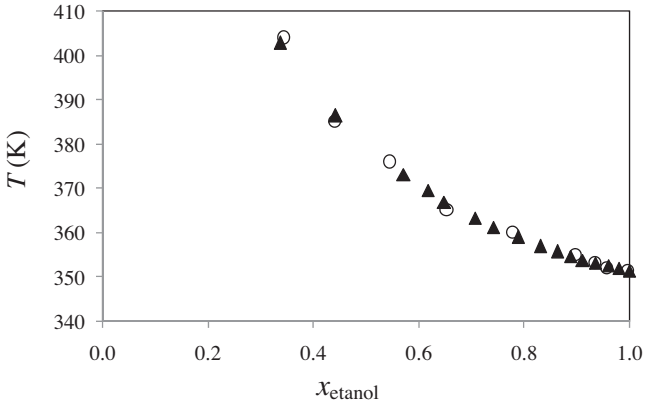

FIGURE 10. Vapor temperature vs. ethanol mole fraction for the system ethanol + [emim][$EtSO_4$]. This work (○), Calvar *et al.* [32] (▲).

TABLE 7
Properties used in the modeling.

Compound	*MM*	*Tc* (K)	*Pc* (MPa)	ω	COSMO[c] segments	V^{COSMO} (Å³)[c]
Methyl acetate[a]	74.08	506.55	4.75	0.33126	459	97.0419
Ethyl acetate[a]	88.11	523.30	3.88	0.36641	571	117.9393
Propyl acetate[a]	102.13	549.73	3.36	0.38890	676	139.8076
m-2-HEAB[b]	163.21	760.26	2.69	1.04756	969	225.8936

[a] Reference [30].
[b] Reference [31].
[c] This work.

nol < m-2-HEAB). In this way, the σ-profile with high values at $\sigma = 0$ show more repulsive interactions between polar and non-polar segments, affecting the cohesive properties of the molecule. The same idea can be applied to mixtures of compounds with very different σ-profiles, *i.e.*, the binary mixture water + m-2-HEAB is the more non ideal system studied here. Interestingly, high deviations of the predicted density can be observed for the aqueous systems at high concentrations of m-2-HEAB, as showed in figure 9. The thermodynamic model was used with the value of the interaction parameters set as zero. The physical properties used in the model for all substances are reported in table 7. The predictive results show percentage relative deviations for the mixtures of m-2-HEAB with water, methanol and ethanol as 0.8%, 1.0%, and 1.0%, respectively. This suggests that σ-profile is an adequate a priori parameter to characterize quantitatively the non-ideality of volumetric behavior.

5.3. VLE data

In order to validate the technique, experimental VLE data for the system ethanol (1) + 1-ethyl-3-methylimidazolium ethylsulfate, [emim] [$EtSO_4$] (2) were determined and compared with published data by Calvar *et al.* [32]. This comparison is shown in figure 10. From the results in this figure, the experimental technique can be considered as validated and can be used to determine the new experimental data involving m-2-HEAB. The same equipment and technique was used in a previous work [33] to obtain VLE data for the binary mixtures [emim] [$EtSO_4$] + (propionaldehyde or valeraldehyde).

Vapor–liquid equilibrium for the binary systems ester (1) + m-2-HEAB (2) has been determined at 101.3 kPa and the results are

TABLE 8
Vapor liquid equilibria at 101.3 kPa for the binary mixtures.

Methyl acetate + m-2-HEAB		Ethyl acetate + m-2-HEAB		Propyl acetate + m-2-HEAB	
x_1	T (K)	x_1	T (K)	x_1	T (K)
1.0000	330.1	1.0000	349.8	1.0000	374.0
0.9746	330.2	0.9612	350.0	0.9575	374.4
0.9004	331.1	0.8956	350.3	0.9283	374.6
0.7753	332.0	0.8294	351.2	0.8944	374.8
0.6889	333.1	0.8188	351.4	0.8446	375.7
0.6174	334.6	0.7904	351.4	0.7410	377.1
0.6137	334.9	0.7576	351.9	0.7207	376.7
0.5399	337.8	0.7312	352.2	0.7153	377.5
0.4938	342.2	0.6925	353.0	0.6922	378.2
0.4872	342.6	0.6824	353.9	0.6616	378.6
0.4798	343.6	0.6581	353.3	0.6423	379.2
0.4696	344.2	0.6419	354.2	0.6289	379.7
		0.6248	354.7	0.6171	380.4
		0.5867	355.3	0.5827	381.6
		0.5807	355.9	0.5548	382.9
		0.5718	357.0	0.5482	383.7
		0.5363	358.3	0.5333	383.3
		0.4995	361.9	0.5121	385.3
		0.4974	361.0	0.4579	389.2
		0.4915	363.4	0.4253	391.3
		0.4558	368.2	0.4040	394.8
		0.4554	365.5	0.4106	393.7
		0.4471	367.3	0.3803	396.8
		0.4339	370.8	0.3653	398.4
		0.4190	371.6	0.3502	400.3
		0.4162	372.7		
		0.3938	374.7		
		0.3780	376.3		
		0.3663	378.8		
		0.3439	379.6		
		0.3423	380.2		

Standard uncertainties u are $u(x) = 0.0008$ and $u(T) = 0.01$ K.

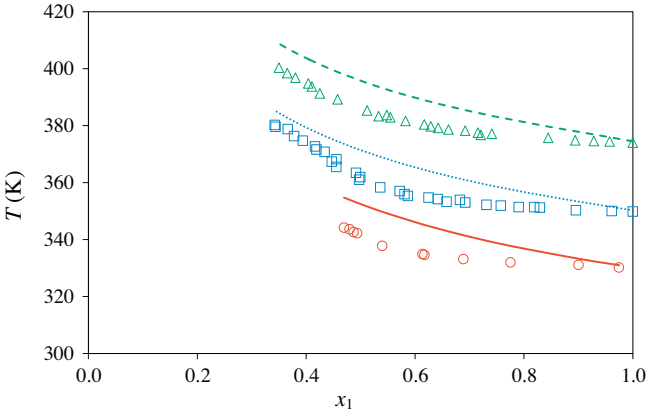

FIGURE 11. Temperature vs. ester mole fraction. (○) methyl acetate (1) + m-2-HEAB (2), (□) ethyl acetate (1) + m-2-HEAB (2), (Δ) propyl acetate (1) + m-2-HEAB (2), and predicted values (solid lines).

summarized in table 8. The experimental data and predicted results for the systems are shown in figure 11 and the percentage average relative deviations for the mixtures of [emim][$EtSO_4$] with methyl acetate, ethyl acetate and propyl acetate are 2.5%, 1.9% and 1.9%, respectively. The representation of the phase behavior has a good trend and the pure vapor phase is correctly predicted for all mixtures.

6. Conclusions

Density and refraction index of binary mixtures ester (methyl acetate or ethyl acetate or propyl acetate) + N-methyl-2-hydroxyethylammonium butyrate (m-2-HEAB) have been measured at atmospheric pressure. Other properties, such as excess molar volume and deviations in the refraction index were also calculated. The values of V^E are negative at high concentrations of ester and positive in the opposite case.

The densities for methyl acetate + m-2-HEAB, ethyl acetate + m-2-HEAB and propyl acetate + m-2-HEAB binary systems have been predicted using the Peng–Robinson equation of state coupled with the Wong–Sandler mixing rule using the COSMO-SAC activity coefficient model. COSMO-SAC is also revealed as a valuable computational tool to describe the intermolecular interaction of systems containing m-2-HEAB. In addition, the σ-profile is suggested as a simple molecular parameter to characterize the non ideality of the mixtures respect to volumetric properties.

The vapor–liquid equilibrium of binary systems ester (methyl acetate, ethyl acetate or propyl acetate) + N-methyl-2-hydroxyethylammonium butyrate at 101.3 kPa was measured by a dynamic method. The experimental density and VLE data were also predicted by using the Peng–Robinson equation of state with the Wong–Sandler mixing rule and the COSMO-SAC model. The prediction results for density are reliable, with deviations <1%, while for the VLE they are only reliable for a qualitative description.

Acknowledgments

V.H. Alvarez acknowledges the financial support from FAPESP (Fundação de Amparo à Pesquisa do Estado de São Paulo), grant 2006/03711-1. M. Aznar is the recipient of a CNPq (Brazil) fellowship.

Appendix A. Supplementary data

Supplementary data associated with this article can be found, in the online version, at http://dx.doi.org/10.1016/j.jct.2013.02.022.

References

[1] R.C. Larock, Comprehensive Organic Transformations, VCH, New York, 1999.
[2] H.-P. Zhu, F. Yang, J. Tang, M.-Y. He, Green Chem. 5 (2003) 38–39.
[3] J.G. Huddleston, H.D. Willauer, R.P. Swatloski, A.E. Visser, R.D. Rogers, Chem. Commun. (1998) 1765–1766.
[4] S. Zhang, Q. Zhang, Z.C. Zhang, Ind. Eng. Chem. Res. 43 (2004) 614–622.
[5] K.N. Marsh, J.A. Boxall, R. Lichtenthaler, Fluid Phase Equilib. 219 (2004) 93–98.
[6] S. Gabriel, J. Weiner, Ber. Dtsch. Chem. Ges. 21 (1888) 2669–2679.
[7] D.F. Kennedy, C.J.J. Drummond, Phys. Chem. B 113 (2009) 5690–5693.
[8] N.J. Bicak, Mol. Liq. 116 (2005) 15–18.
[9] T.L. Greaves, A. Weerawardena, C. Fong, I. Krodkiewska, C.J.J. Drummond, Phys. Chem. B 110 (2006) 22479–22487.
[10] I. Cota, R. González-Olmos, M. Iglesias, F.J. Medina, Phys. Chem. B 111 (2007) 12468–12477.
[11] K. Kurnia, C. Wilfred, T.J. Murugesan, Chem. Thermodyn. 41 (2009) 517–521.
[12] V.H. Alvarez, N. Dosil, R. Gonzalez-Cabaleiro, S. Mattedi, M. Martin-Pastor, M. Iglesias, J.M.J. Navaza, Chem. Eng. Data 55 (2010) 625–632.
[13] M. Iglesias, A. Torres, R. Gonzalez-Olmos, D.J. Salvatierra, Chem. Thermodyn. 40 (2008) 119–133.
[14] J. Sierra, E. Martí, A. Mengíbar, R. González-Olmos, M. Iglesias, R. Cruañas, M.A. Garau, 5th Society of Environmental Toxicology and Chemistry Congress – SETAC 2008, Sydney, 2008.
[15] B. Peric, E. Martí, J. Sierra, R. Cruañas, M. Iglesias, M.A. Garau, Environ. Toxicol. Chem. 30 (2011) 2802–2809.
[16] L. Sarkar, M.N. Roy, Thermochim. Acta 496 (2009) 124–128.
[17] D. Peng, D.B. Robinson, Ind. Eng. Chem. Fundam. 15 (1976) 59–64.
[18] V.H. Alvarez, M.J. Aznar, Chin. Inst. Chem. Eng. 39 (2008) 353–360.
[19] D.S.H. Wong, S.I. Sandler, AIChE J. 38 (1992) 671–680.
[20] D.S. Abrams, J.M. Prausnitz, AIChE J. 21 (1975) 116–128.
[21] S.T. Lin, S.I. Sandler, Ind. Eng. Chem. Res. 41 (2002) 899–913.
[22] Accelrys Materials Studio, <http://accelrys.com/products/materials-studio/>, accessed January 2010.
[23] E. Mullins, R. Oldland, Y.A. Liu, S. Wang, S.I. Sandler, C.C. Chen, M. Zwolak, K.C. Seavey, Ind. Eng. Chem. Res. 45 (2006) 4389–4415.
[24] M. Diedenhofen, A. Klamt, Fluid Phase Equilib. 294 (2010) 31–38.
[25] A. Peneloux, E. Rauzy, R. Freze, Fluid Phase Equilib. 8 (1982) 7–23.
[26] V.H. Alvarez, S. Mattedi, M. Aznar, Ind. Eng. Chem. Res. 44 (2012) 14543–14554.
[27] M.L. Michelsen, J. Mollerup, Thermodynamic Models: Fundamentals and Computational Aspects, second ed., Tie-Line Publications, Lyngby, 2007.
[28] V.H. Alvarez, R. Larico, Y. Ianos, M. Aznar, Braz. J. Chem. Eng. 25 (2008) 409–418.
[29] M. Nakata, M.J. Sakurai, Chem. Soc. Faraday Trans. 83 (1987) 2449–2457.
[30] Diadem Public 1.2, The DPPR Information and Data Evaluation Manager, 2000.
[31] J.O. Valderrama, P.A. Robles, Ind. Eng. Chem. Res. 46 (2007) 1338–1344.
[32] N. Calvar, B. González, E. Gómez, Á.J. Dominguez, Chem. Eng. Data 53 (2008) 820–825.
[33] V.H. Alvarez, S. Mattedi, M.J. Aznar, Chem. Thermodyn. 43 (2011) 895–900.

JCT 12-405